Environ Monit Assess (2010) 167:265–288
DOI 10.1007/s10661-009-1048-9

Seasonal variation, source, and regional representativeness of the background aerosol from two remote sites in western China

Wenjun Qu · Dan Wang · Yaqiang Wang · Lifang Sheng · Gang Fu

Received: 28 December 2008 / Accepted: 4 June 2009 / Published online: 25 July 2009

Abstract Using observations from two remote sites during July 2004 to March 2005, we show that at Akdala (AKD, 47° 06′ N, 87° 58′ E, 562 m asl) in northern Xinjiang Province, there were high wintertime loadings of organic carbon (OC), elemental carbon (EC), and water-soluble (WS) SO_4^{2-}, NO_3^{2-}, and NH_4^+, which is similar to the general pattern in most areas of China and East Asia. However, at Zhuzhang (ZUZ, 28° 00′ N, 99° 43′ E, 3,583 m asl) in northwestern Yunnan Province, the aerosol concentrations and compositions showed little seasonal variation except for a decreasing trend of OC from August to autumn–winter. Additionally, the OC variations dominated the seasonal variation of PM_{10} (particles $\leq$10 μm diameter) level. Chemical characteristics combined with transport information suggested sea salt origin of ionic Na^+, Mg^{2+}, and Cl^- at ZUZ. At AKD, ionic Ca^{2+}, Mg^{2+}, Na^+, and Cl^- primarily originated from salinized soil. Furthermore, the WS Ca^{2+} contributions (5.4–6%) to the PM_{10} mass during autumn, winter, and early spring reflected a constant dust component. The results of this study indicated that both sites were regionally representative. However, the representative regions and scales of these background sites may vary seasonally as the regional atmospheric transport patterns change. Seasonal variations in the background aerosol levels from these two areas need to be considered when evaluating the regional climate effects of the aerosols.

Keywords Atmospheric aerosol background · Regional representativeness · Seasonal variation and source · Zhuzhang (ZUZ) and Akdala (AKD) · Southwestern and northwestern China

W. Qu (✉) · L. Sheng · G. Fu
Key Laboratory of Physical Oceanography, Ocean-Atmosphere Interaction and Climate Laboratory, Department of Marine Meteorology, College of Physical and Environmental Oceanography, Ocean University of China, Qingdao 266100, People's Republic of China
e-mail: quwj@ouc.edu.cn, quwj@163.com

W. Qu · Y. Wang
Key Laboratory of Atmospheric Chemistry, Centre for Atmosphere Watch and Services (CAWAS), Chinese Academy of Metrological Sciences, China Meteorological Administration, Beijing 100081, People's Republic of China

D. Wang
State Key Laboratory of Loess and Quaternary Geology, Institute of Earth Environment, Chinese Academy of Sciences, Xi'an 710075, People's Republic of China

Introduction

Atmospheric aerosols vary greatly over time and space; therefore, accurate depictions of both the average aerosol loadings and their variability are

important for understanding their large-scale impacts on global climate systems. Data representative of regional or global aerosol levels are more valuable in this context. Observations made at certain remote sites in which the influences of local pollutants are minimal and conditions are representative of a large area are expected to provide reasonable representations of a well-mixed atmosphere and are thus potentially suitable for the analysis of background aerosol conditions (Hidy and Blanchard 2005). However, because it is difficult to ensure that a site is free of pollution disturbances, the regional representativeness of the aerosols collected at such *background* sites must be considered carefully. For example, Blanchard et al. (1999) investigated the spatial representativeness and scales of transport for primary particulate and gas-phase precursors of secondary aerosols in San Joaquin Valley, CA, USA.

Although observations have been made for decades at Chinese background sites, background aerosol data are still limited in China. Past observations primarily targeted long-term variations of gaseous species (Wang et al. 2002; Zhou et al. 2004), while observations of atmospheric aerosols have mostly been short term and involved trace elements and WS ions (Ma et al. 2003; Wang et al. 2004). Furthermore, to the authors' knowledge, atmospheric background observations were not made in remote southwestern and northwestern China until 2004 (Qu et al. 2008).

Study has been conducted at two China Atmosphere Watch Network (CAWNET) sites, Zhuzhang (ZUZ) and Akdala (AKD, Fig. 1),

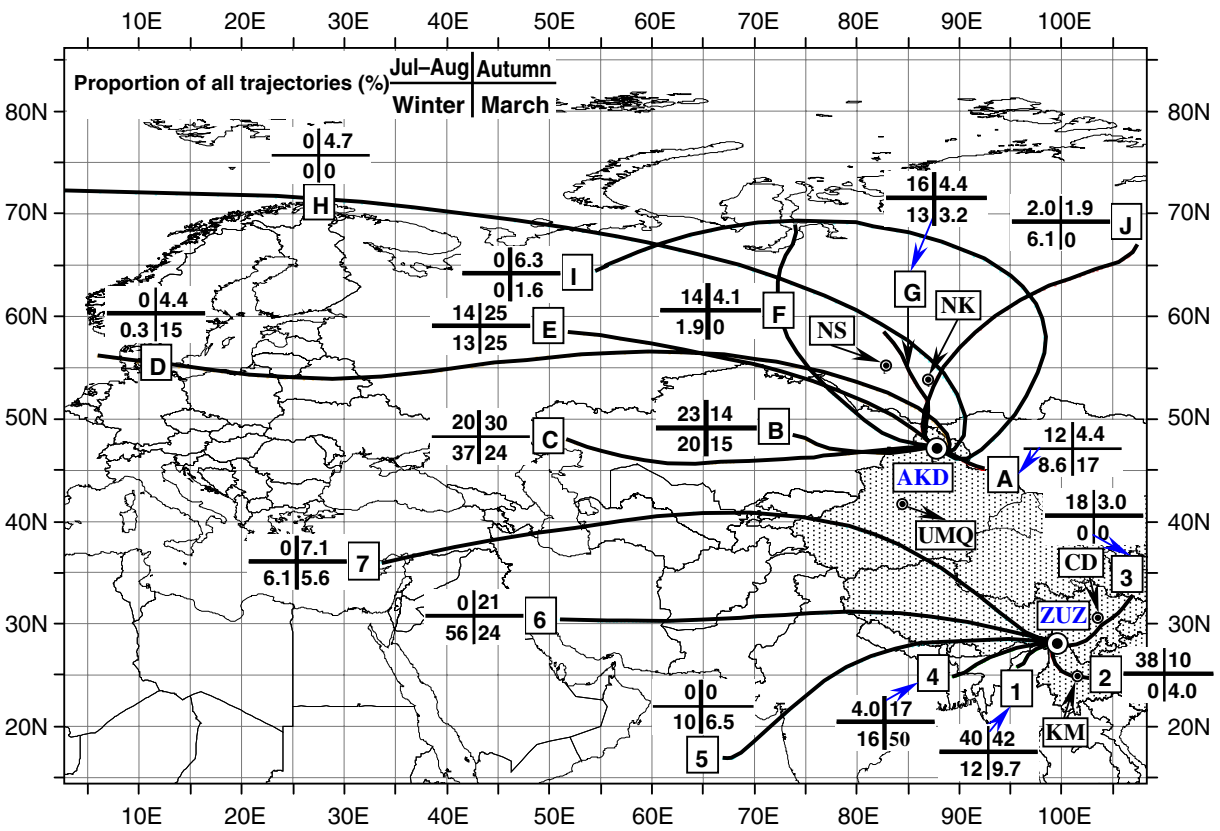

Fig. 1 Sampling sites and 5-day backward trajectory clusters for Zhuzhang (*ZUZ*; cluster 1–7) and Akdala (*AKD*; cluster A–J). The *shadowed area* represents continental China. *NK*, *NS*, *UMQ*, *CD*, and *KM* denote Novokuznetsk, Novosibirsk, Urumqi, Chengdu, and Kunming, respectively. The proportions of every trajectory cluster in all the trajectories during different seasons are also presented (adapted after Qu et al. 2008)

to assess regional aerosol backgrounds. We have described the aerosol composition and influences from regional transport previously (Qu et al. 2008). In the present paper, we (1) evaluate meteorological influences on the aerosol concentration and characterize the seasonal variation of the aerosol populations; (2) identify possible sources of the aerosol species based on their chemical characteristics, variation, and inter-relationships as well as information regarding their transport; (3) assess the spatial representativeness of the two sites.

Methods

The atmospheric aerosol composition was measured at two remote CAWNET sites: (1) ZUZ (28° 00′ N, 99° 43′ E, 3583 m asl, on the southeast margin of the Tibetan Plateau) and (2) AKD (47° 06′ N, 87° 58′ E, 562 m asl, on the north margin of the Zhungaer Basin, Fig. 1). Because the sampling and analysis techniques have been described previously (Qu et al. 2008), only a brief description is given below. From July 2004 to March 2005, 72-h (normally from 8:00 to 8:00) bulk PM_{10} (particles $\leq$10 μm) samples were collected at both ZUZ and AKD. Meanwhile, daytime (normally from 8:00 to 20:00) bulk TSP (total suspended particle) samples were also collected but only at AKD. Whatman quartz microfiber filters (47 mm diameter; QM/A, Whatman, Maidstone, UK; preheated at 800°C for 4 h to remove contaminants) were used for sampling except for the first 2 weeks when 47-mm-diameter Teflon™ (PTFE) filters (WTP, Whatman) were used. An electronic microbalance with a sensitivity of 1 μg (ME 5-F, Sartorius AG, Goettingen Germany) was used to gravimetrically determine the aerosol mass. The aerosol-laden filters were stored in Petri dishes enclosed in plastic bags at 4°C after sampling until chemical analysis was conducted.

The bulk samples were analyzed for organic carbon (OC)/elemental carbon (EC) using a DRI Model 2001 Thermal/Optical Carbon Analyzer following the IMPROVE thermal/optical reflectance procedure (Chow et al. 1993). The water-soluble (WS) ions, including SO_4^{2-}, NO_3^-, NH_4^+, Ca^{2+}, Mg^{2+}, K^+, Na^+, NO_2^-, Cl^-, and F^-, were measured using a Dionex 600 ion chromatograph equipped with an electrochemical detector (Dionex ED50A). A proton-induced X-ray emission method was used to determine the concentrations of selected trace elements, including As, Br, Ca, Cl, Cr, Cu, Fe, K, Mn, Ni, Pb, S, Se, Sr, Ti, V, Zn, and Zr for quartz filters and an additional four elements (Al, Mg, P, Si) for Teflon™ filters. All data were corrected for backgrounds based on the average of the blank filters (Qu et al. 2008).

Because information of transport was helpful for identification of possible sources of the aerosol populations and evaluation of the regional representativeness of the observation sites, hierarchical clustering results of the 5-day air mass backward trajectories to ZUZ and AKD (Qu et al. 2008) were also used in this study. The trajectories were calculated four times each day (00, 06, 12, and 18 UTC) using the NOAA HYSPLIT4 trajectory model (Draxler and Hess 1998) and then divided into distinct transport clusters by a multivariate statistical analysis method—trajectory clustering analysis (Moody and Galloway 1988; Arimoto et al. 1999). National Center for Environmental Prediction FNL (final analysis) meteorological field data were used in trajectory calculation, while Ward's method was used to create hierarchical clusters, and the squared Euclidean distances were used to determine the similarities between the trajectories. It is worth noting that errors of 20% of the distance traveled appear to be typical for trajectories computed from analyzed wind fields (Stohl 1998). The aerosol transport pathways to ZUZ and AKD (Fig. 1) are briefly summarized in Table 1. Detailed information regarding the transport pathways can be found in Qu et al. (2008).

Principal component analysis (PCA) is widely used to reduce data (Loska and Wiechuya 2003) and extract a small number of latent factors (principal components, PCs) for assessment of the associations (relationships) among the observed aerosol species. PCA is often used as an explanatory tool to identify the major sources of air pollutant emissions. The PCA with VARIMAX normalized rotation, which can maximize the variances of the factor loadings across variables for each factor, was applied in this study. As suggested by the Kaiser criterion (Kaiser 1960),

Table 1 Aerosol transport pathways to Zhuzhang (ZUZ) and Akdala (AKD)

Types of transport pathways		Trajectory clusters included, source regions, and potential sources
Zhuzhang (ZUZ)	The polluted trajectories	The northeasterly Cluster 3 (C-3) from the Sichuan Basin with extensive emissions from coal-combustion and mining
		The southeasterly C-2 passed over southeastern Yunnan Province
	Clean transport pathways	The southwesterly C-1 and C-4 pathways from coastal regions near the Bay of Bengal (with comparatively low loadings of aerosol species)
	Remote clean pathways	The southwesterly C-5 from the Arabian Sea, the westerly C-6 from West Asia, and northwesterly C-7 from East Europe (with relatively low pollutant burdens)
Akdala (AKD)	The major pathways for air pollutants	The northeasterly C–J and northwesterly C–G passing near major Russian industrial cities (NK—Novokuznetsk and NS—Novosibirsk) with steel production, metallurgy, coal mining, and petroleum as potential sources
		The southeasterly C–A passed over the boundary area between northwestern China and Mongolia with extensive coal and metal mining operations
	Clean transport pathways	The northwesterly C–H, C–I, and C–F pathways (for clean air) from high latitude areas in eastern Europe and Russia
	Dust influenced trajectories	The westerly C–B, C–C, C–D, and C–E trajectories, influenced by salinized dust delivered by the prevailing winds from the Gobi, sandy lands, and deserts in eastern Kazakhstan and in the area

only those components with eigenvalues >1.0 were retained in this study because they can account for a meaningful amount of variance.

Three approaches were applied to identify the likely sources of the aerosol species: examination of chemical characteristics, variation and inter-correlations among the species combined with information regarding their transport, calculation of the EF_{crust} {enrichment factor calculated relative to crustal rock, EF_{crust} = (Element/Fe)air/(Element/Fe)crust, using the upper continental crust composition compiled by Taylor and McLennan 1995} of the elements, and PCA.

Results

Characterization of the well-mixed aerosols at ZUZ and AKD

OC and EC, WS SO_4^{2-}, NH_4^+, Na^+, and Mg^{2+}, and elemental S and K generally exhibited synchronous variations throughout the course of the study at ZUZ (not shown). In addition, good correlations were observed between SO_4^{2-}, NH_4^+, and K^+ in ZUZ PM_{10} samples (Fig. 4a and b), and these ions were generally anthropogenic origin. At AKD, similar variations were also observed for OC and EC and WS SO_4^{2-} and NH_4^+; meanwhile, elemental Ca, Ti, Fe, and K also varied synchronously during the early period of the study when element measurements were available (not shown). EC showed significant correlations with SO_4^{2-} and K^+ in AKD PM_{10} samples (Fig. 4c), which suggests that there were contributions from coal combustion and biomass burning, two possible major sources of anthropogenic emissions in the region. Furthermore, there was a strong correlation between NH_4^+ and SO_4^{2-} (Fig. 4d), which likely resulted from their coexistence as ammonium sulfate/bisulfate particles. However, significant correlations were also observed between NO_3^-, K^+, and SO_4^{2-} (apparently from different origins) at AKD.

It is worth noting that the good inter-correlations between these aerosol species at ZUZ and AKD do not necessarily indicate that they originated from an identical source. In fact, this may reflect their covariation as a result of synoptic processes and mixing during regional transport. Because our study sites were far from residential areas and other sources of pollution,

the observed results may not have been due much to proximate sources. Measurements of the aerosols at these remote sites can thus be regarded as indicators of regional atmospheric backgrounds that reflect the average conditions of regional transported and well-mixed pollutants from various sources. The arithmetic mean concentrations of the major aerosol species at ZUZ and AKD are shown in Figs. 2 and 3.

Moreover, the SO_4^{2-}/EC ratio was 12 for most of the samples ($n = 34$), larger than that ratio (5.0) for 12 other samples (Fig. 4c). This may reflect the influence of coal combustion on most of the sampling days. The K^+/EC ratio and SO_4^{2-}/EC ratio shown in Fig. 4c may be regarded as characteristic of different types of regional emissions. Additionally, EC also correlated well with elemental S ($r = 0.63$, $n = 22$, $p < 0.01$ significance) in the AKD TSP samples, probably due to the contribution from coal combustion.

Carbonaceous aerosol at ZUZ and AKD

EC and total carbon (TC) in the PM_{10} varied synchronously at low levels, with no pronounced seasonality at ZUZ, while semi-volatile organic carbon (SVOC), which is the organic carbon that evolved from the filter punch in the He-only atmosphere at 120°C during analysis, showed a summer to winter decrease. Because other SVOC sources are limited in such a background region, this distinct seasonality in SVOC levels suggest the contribution of biogenic source such as the flourishing vegetation during summer and autumn (Qu et al. 2008). Geron et al. (2006) has verified biogenic sources of isoprene from the forest floor and canopy in this region. OC dominated the ZUZ carbonaceous aerosols in PM_{10} with a contribution to TC that fluctuated around 90%, while only ~10% of the TC was composed of EC. In addition, OC variability was large in

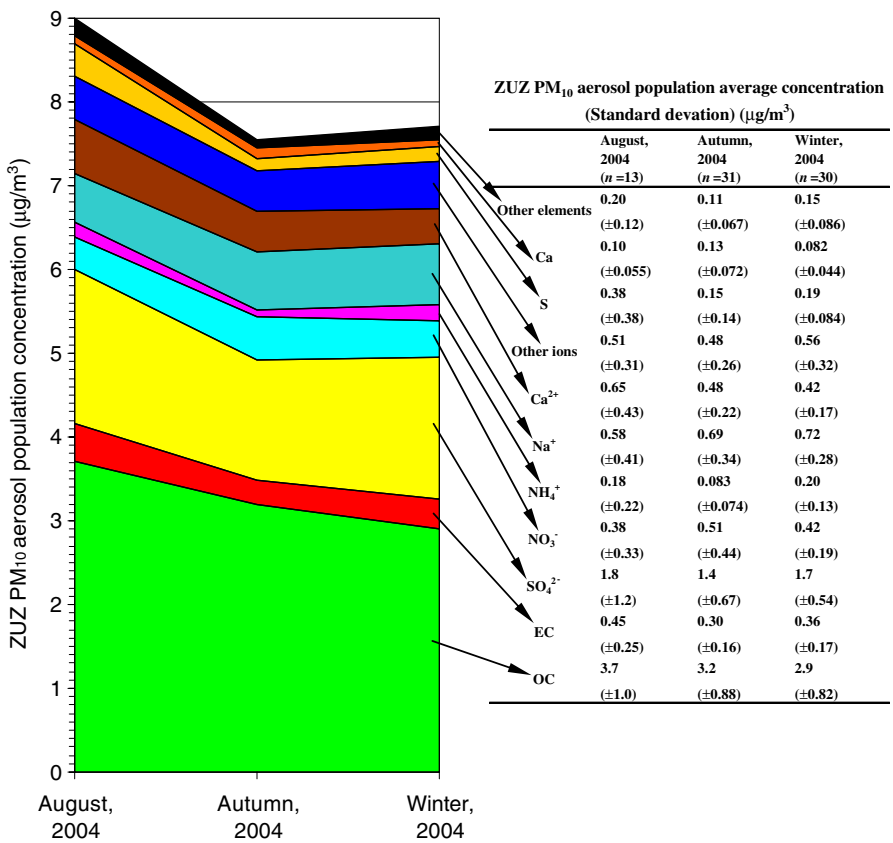

ZUZ PM_{10} aerosol population average concentration (Standard devation) (µg/m³)

	August, 2004 (n =13)	Autumn, 2004 (n =31)	Winter, 2004 (n =30)
Other elements	0.20 (±0.12)	0.11 (±0.067)	0.15 (±0.086)
Ca	0.10 (±0.055)	0.13 (±0.072)	0.082 (±0.044)
S	0.38 (±0.38)	0.15 (±0.14)	0.19 (±0.084)
Other ions	0.51 (±0.31)	0.48 (±0.26)	0.56 (±0.32)
Ca^{2+}	0.65 (±0.43)	0.48 (±0.22)	0.42 (±0.17)
Na^+	0.58 (±0.41)	0.69 (±0.34)	0.72 (±0.28)
NH_4^+	0.18 (±0.22)	0.083 (±0.074)	0.20 (±0.13)
NO_3^-	0.38 (±0.33)	0.51 (±0.44)	0.42 (±0.19)
SO_4^{2-}	1.8 (±1.2)	1.4 (±0.67)	1.7 (±0.54)
EC	0.45 (±0.25)	0.30 (±0.16)	0.36 (±0.17)
OC	3.7 (±1.0)	3.2 (±0.88)	2.9 (±0.82)

Fig. 2 Seasonal variation of organic carbon (*OC*), elemental carbon (*EC*), water-soluble (*WS*) ions, and selected trace elements in PM_{10} at ZUZ. Other ions included K^+, Mg^{2+}, F^-, Cl^-, and NO_2^-; other elements included As, Br, Cl, Cr, Cu, Fe, K, Mn, Ni, Pb, Se, Sr, Ti, V, Zn, and Zr

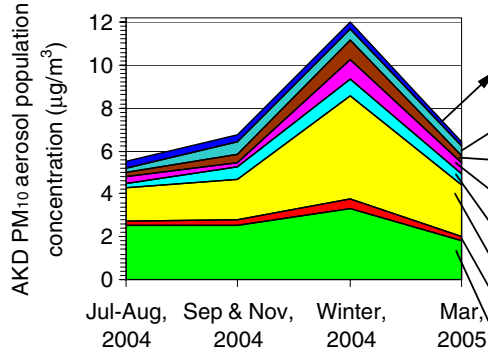

AKD PM_{10} aerosol population average concentration (±Standard devation) (μg/m^3)

	Jul-Aug, 2004 (n =14)	Sep & Nov, 2004 (n =10)	Winter, 2004 (n =27)	Mar, 2005 (n =6)
Other ions	0.28 (±0.17)	0.37 (±0.21)	0.35 (±0.13)	0.18 (±0.068)
Na^+	0.25 (±0.23)	0.53 (±0.19)	0.53 (±0.12)	0.46 (±0.071)
Ca^{2+}	0.17 (±0.13)	0.45 (±0.52)	0.91 (±1.4)	0.36 (±0.16)
NH_4^+	0.31 (±0.17)	0.19 (±0.24)	0.87 (±0.34)	0.49 (±0.28)
NO_3^-	0.23 (±0.23)	0.53 (±0.71)	0.79 (±0.26)	0.53 (±0.26)
SO_4^{2-}	1.5 (±0.54)	1.9 (±1.4)	4.8 (±1.8)	2.4 (±1.5)
EC	0.19 (±0.066)	0.25 (±0.31)	0.45 (±0.32)	0.16 (±0.049)
OC	2.5 (±0.83)	2.5 (±1.3)	3.3 (±1.8)	1.8 (±0.13)

Fig. 3 Seasonal variation of organic carbon (*OC*), elemental carbon (*EC*), water-soluble (*WS*) ions, and selected trace elements in PM_{10} at AKD. Other ions included K^+, Mg^{2+}, F^-, Cl^-, and NO_2^-; other elements included As, Br, Cl, Cr, Cu, Fe, K, Mn, Ni, Pb, Se, Sr, Ti, V, Zn, and Zr

summer and autumn (2.2–6.2 μg m^{-3}) than in winter (1.5–4.7 μg m^{-3}), which was likely due to the more favorable conditions for SVOC emission and for secondary organic carbon (SOC) transformation during summer and autumn. Note here that SOC was determined based on OC/EC ratio, that is, $SOC = OC - (OC/EC)_{min} \times EC$ (Castro et al. 1999).

PM_{10} TC at ZUZ was well correlated with high temperature organic carbon (HTOC), OC, and EC, but not with SVOC (Fig. 5a and b), which suggests that HTOC, OC, and EC were constant

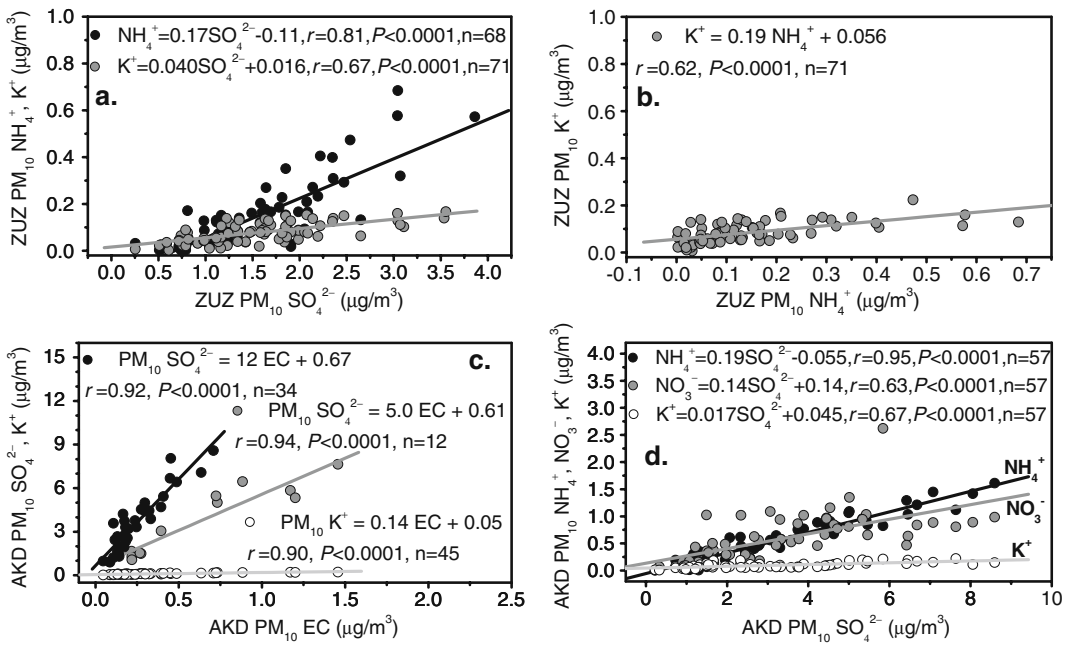

Fig. 4 Linear correlation between ionic NH_4^+, K^+, and SO_4^{2-} (**a**) between ionic K^+ and NH_4^+ (**b**) in PM_{10} at Zhuzhang (*ZUZ*); linear correlation between ionic SO_4^{2-}, K^+, and elemental carbon (*EC*; **c**), between ionic NH_4^+, NO_3^-, K^+, and SO_4^{2-} (**d**) in PM_{10} at Akdala (*AKD*). The good inter-correlations between the aerosol populations apparently from different sources indicate their synchronous variations, suggesting well mixing of these aerosol components during synoptic process and regional transport

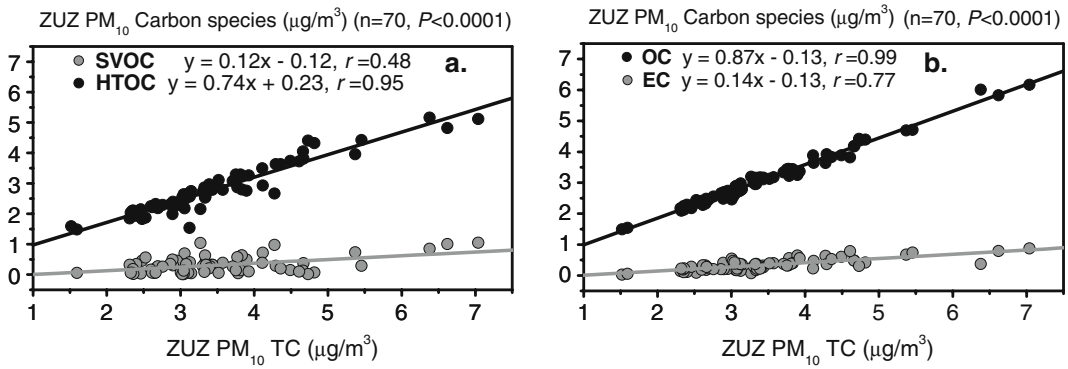

Fig. 5 Correlations between semi-volatile organic carbon (*SVOC*), high temperature organic carbon (*HTOC*), and total carbon (*TC*) concentrations (**a**) between organic carbon (*OC*), elemental carbon (*EC*), and TC concentrations (**b**) in PM_{10} at Zhuzhang (*ZUZ*) during August 2004–February 2005

TC components. Here, HTOC is the carbon fractions that evolved from the filter punch in a He-only atmosphere at 250°C, 450°C, and 550°C plus the pyrolyzed organic carbon during the analysis, which is equal to OC minus SVOC. SVOC was quite variable, which may have been due to changing meteorological conditions. Indeed, the highly variable weather during summer and autumn at ZUZ may result in variations in solar radiation, ambient/ground temperature, and soil humidity, which can influence SVOC emission from the vegetation and soil.

At AKD, PM_{10} OC and EC varied synchronously, with evidently high concentrations occurring during winter (similar to WS SO_4^{2-}); this was likely due to increased anthropogenic emissions from domestic heating (Qu et al. 2008). The variations of OC, EC, and SO_4^{2-} levels also increased during winter, as indicated by ranges of 1.8–10.1, 0.12–1.5, and 2.0–8.6 μg m^{-3}, respectively, during winter, and 1.7–3.8, 0.087–0.27, and 0.73–2.8 μg m^{-3}, respectively, during summer. Moreover, OC and EC contributed ~93% and ~6.9% of the PM_{10} TC in August versus ~88% and ~12% during winter. And, the average OC and EC contributions to the TSP TC were ~92% and ~7.9% from July to September.

Meteorological influences on the aerosol concentration

Meteorological conditions can influence the aerosol concentration in different ways. For example, the convection intensity can influence the diffusion and dilution of the pollutants, precipitation can result in wet scavenging of the particles, and the formation of secondary aerosols as a result of gas/particle conversion of precursor gases (photochemical activity) can be influenced by solar radiation, ambient temperature, humidity, and the concentrations of oxidants such as O_3.

Statistics of the August-autumn surface wind at ZUZ indicated that the 24 h and 14:00 (local time, normally the most intensive convection period in a day) mean wind velocities for EC polluted days (EC concentration > median EC concentration) were 0.92 and 1.58 m/s, respectively. Conversely, these values were 1.16 and 1.90 m/s, respectively, on EC clean days (EC concentration < median EC concentration). A comparison of the wind velocities for OC polluted and OC clean days was similar. That is, high OC and EC levels were found to be associated with weak wind and convection, which generally enables pollutants to accumulate in the lower boundary layer. Moreover, high OC levels during weak convection periods may also result from more sufficient SOC transformation due to the prolonged stagnation of the precursor gases in a comparatively stable atmosphere. A strong southwest wind vector was observed for EC clean days in the surface wind rose (not shown), which likely reflects the contribution of the clean southwesterly trajectories (cluster C-1 and C-4) from coastal regions near the Bay of Bengal (Fig. 1, Table 1).

PM_{10} measurement at ZUZ exhibited higher levels of OC and EC (3.3 and 0.35 μg m^{-3}) on non-precipitation days (compared with 2.8 and 0.33 μg m^{-3} on precipitation days), probably due to the absence of wet scavenging. However, on non-precipitation days, meteorological conditions became more favorable for more efficient SOC formation from precursor gases and for increased SVOC emission from natural sources (e.g., vegetation and soil), which also contributed to higher OC levels then. Moreover, a unique ~1-week fluctuation of filterable NO_3^- in PM_{10} (averaging 0.55 μg m^{-3} on sunny and partly cloudy days versus 0.36 μg m^{-3} on rainy and cloudy days) at ZUZ was attributed to variation in the photochemical transformation of NO_χ and formation of NO_3^- in response to meteorological conditions such as ambient humidity, temperature, and solar radiation (Qu et al. 2008).

Interestingly, SVOC concentrations in the AKD PM_{10} samples were in two specific ranges with modal values of ~0.2 and ~0.55 μg m^{-3} (Fig. 6a and b). The cause of this SVOC fluctuation pattern (Fig. 6a) remains unclear. However, there was a significant correlation between the SVOC concentration and daily averaged surface temperature (Fig. 6c). These results suggest that the ambient temperature (varying with the weather shift) had an effect on SVOC emission, which was primarily from natural biogenic sources and the evaporation of organic material from soil in remote regions such as AKD.

SOC formation is expected to be more efficient when it is sunny and warm and there are high O_3 levels (Turpin and Huntzicker 1991; Lim 2001). There was a significant correlation between the SOC concentration in AKD PM_{10} and the ambient O_3 concentration (observed synchronously during sampling using a 49C UV Photometric O_3 Analyzer, Thermo Electron, USA; Fig. 6d). Although confined by the limited O_3 data available, this correlation confirms that a high O_3 level is favorable to SOC formation. SOC dominated OC variation (Qu et al. 2009), resulting in a similar significant correlation between the PM_{10} OC concentration and the ambient O_3 level (Fig. 6e).

Seasonal variations of the aerosol populations at ZUZ and AKD

Zhuzhang

At ZUZ, seasonal variations of the individual aerosol populations were not distinct, with the exception of OC, which decreased from August to autumn–winter and dominated the PM_{10} variation (Fig. 2). This decline in OC can be at least partially attributed to reductions in SVOC emission and in SOC transformation that occurred in response to the changing seasons. In summer and autumn, SVOC might have strong source strength due to seasonality in the growth cycles of vegetation; meanwhile, the formation of SOC was likely more efficient when solar radiation favored photochemical activity intensified (Dusek 2000).

The high summertime PM_{10} level may have resulted from the contribution of SVOC and SOC and regional pollutants delivered by the C-3 and C-2 trajectories from vicinal sources to ZUZ (Fig. 1, Table 1). However, in autumn and winter, there was an increased frequency of long-range C-5, C-6, and C-7 trajectories for clean air, the contribution from regional pollutants most likely decreased. The slightly increase of EC, SO_4^{2-}, and NH_4^+ concentrations in winter when compared to autumn may have resulted from the increased regional combustion emissions due to the heating season.

As a remote background site, the efficient mixing upwind, limited local anthropogenic influence, and possible unobvious seasonality in regional emissions probably led to indistinct seasonal variations of the aerosol populations at ZUZ.

Akdala

Evident seasonality was found for OC, EC, SO_4^{2-}, NO_3^{2-}, and NH_4^+ in the AKD PM_{10} samples, with significantly higher levels occurring during winter (Fig. 3). Specifically, the wintertime mean EC concentration was almost twice that of the summer and autumn concentrations, while the winter SO_4^{2-} and NH_4^+ concentrations were almost two to three times those of the summer and autumn.

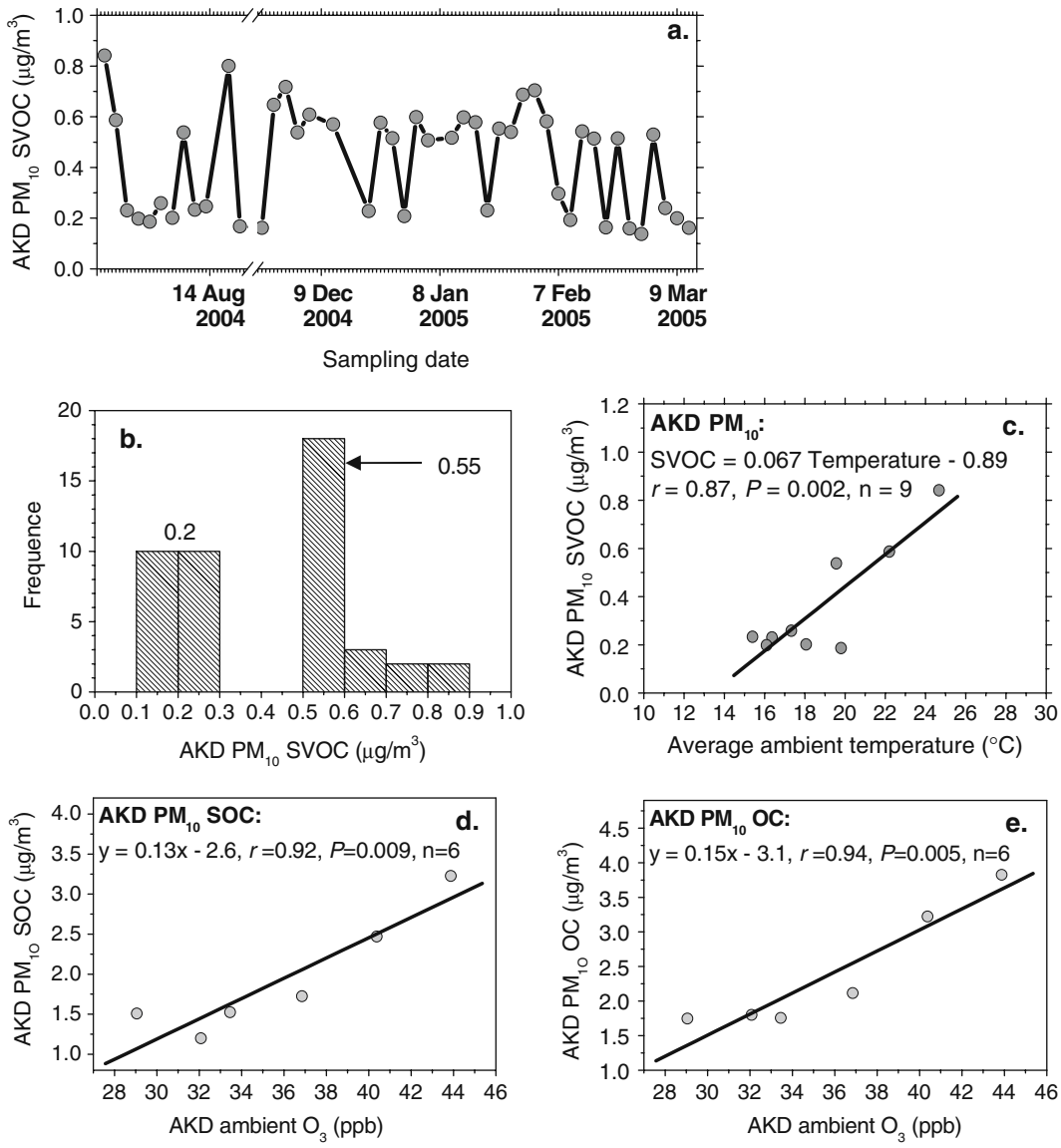

Fig. 6 Time series (**a**) and statistical distribution (**b**) of semi-volatile organic carbon (*SVOC*) concentrations in PM_{10} at Akdala (*AKD*) during August 2004–March 2005 and its relationship with available ambient temperature during middle August–middle September 2004 (**c**); the relationship between PM_{10} secondary organic carbon (*SOC*) concentration (**d**), PM_{10} OC concentration (**e**), and available ambient O_3 concentration in August 2004 at Akdala (*AKD*)

The higher winter loadings of these pollutants were likely due to increased emissions from coal combustion, biomass burning, and other sources of domestic heating in northern Xinjiang Province and neighboring areas.

WS Ca^{2+} has been used as an indicator to evaluate the contribution of mineral dust (Seinfeld et al. 2004; Arimoto et al. 2004). At AKD, although the wintertime mean WS Ca^{2+} concentration was almost two to five times greater than the summer

and autumn concentrations, its fractions in the PM_{10} mass were in an accordant range (5.4–6%) during the whole sampling course except for summer (2.2%). These results suggest that there is a relatively constant dust contribution in autumn, winter, and early spring. Intensive wind during these seasons might lead to enhanced release of crust material in this mid–high latitude area. However, inconsistent with the generally acknowledged intensive springtime dust emission from East Asian sources, the mean PM_{10} Ca^{2+} concentration in March was lower than the concentrations in autumn and winter (Fig. 3), probably due to limited measurements in the spring.

The WS Na^+ and Ca^{2+} concentrations (0.69 and 0.85 μg m^{-3}) were higher than or comparable to the NO_3^- and NH_4^+ concentrations (0.84 and 0.17 μg m^{-3}) in the AKD TSP samples, which was also true for the PM_{10} at AKD and ZUZ (Figs. 2 and 3). These consistent characteristics at ZUZ and AKD differ from the conditions at most urban sites, where sulfate, nitrate, and ammonium are usually major ions in the aerosol (the NO_3^- and NH_4^+ concentrations were only lower than the SO_4^{2-} concentration but often higher than the other ions). Due to the limited local anthropogenic influence on the sites and possible limited regional transport of nitrate and ammonium, which are active in photochemical transformation and efficient in deposition, crustal or marine origin materials might become important aerosol components in these background areas. This would result in the contributions of Na^+ and Ca^{2+} to aerosol WS ions being comparable to the contributions of NO_3^- and NH_4^+.

Difference in the concentration of WS ions between PM_{10} and TSP at AKD

The difference in the concentration of WS ions between PM_{10} and TSP at AKD provides useful information regarding their source (Fig. 7). This comparison was based on comparable numbers of both size samples in August. Most of the ionic Na^+, Mg^{2+}, Ca^{2+}, F^-, Cl^-, NO_2^-, and NO_3^- was present in coarser particles with proportions in the PM_{10} comprising less than 60% of those in the TSP (Fig. 7b). For example, the WS Ca^{2+} in the PM_{10} accounted for only 15% of that in the TSP. The distribution of these ions primarily occurring in coarser particles was consistent with their major crustal origin mentioned before.

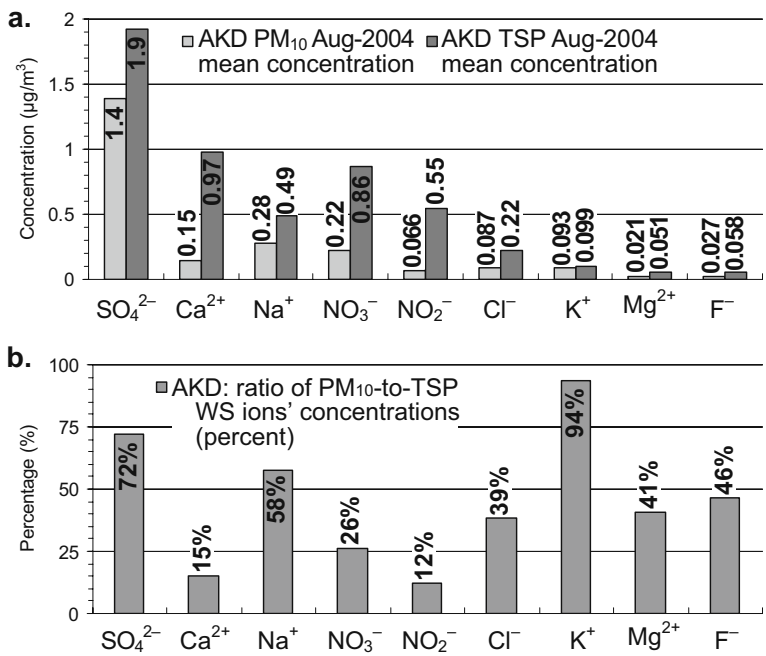

Fig. 7 Comparison of the concentrations of water-soluble (*WS*) ions in PM_{10} and in TSP (**a**); ratio of PM_{10}-to-TSP WS ions' concentrations (percent; **b**) at Akdala (*AKD*)

Conversely, the SO_4^{2-} and K^+ concentrations in the PM_{10} accounted for 72% and 94% of those in the TSP, indicating large proportions in PM_{10}. These findings may indicate the presence of secondary sulfate from coal combustion and K^+ from biomass burning.

In summary, the secondary aerosols from anthropogenic sources (including sulfate and potassic particles) were primarily present in the PM_{10}, while crust origin cations such as Ca^{2+}, Mg^{2+}, and Na^+ were primarily found in the TSP in this region. These findings are similar to the size distribution of aerosol ions in Hungary reported by Krivácsy and Molnár (1998).

Similar variation of the aerosols at ZUZ and AKD to the PM_{10} and SO_2 loads in the regional cities

The concentrations of aerosol populations observed at ZUZ and AKD were compared with the concentrations of pollutants in the regional cities to determine if the results reflected the variations in the regional pollutants. For this comparison, the daily PM_{10} loads in the regional cities were used, including Kunming (KM, 25° 01′ N, 102° 41′ E) and Chengdu (CD, 30° 40′ N, 104° 05′ E), which are located near ZUZ, and Urumqi (UMQ, 43° 47′ N, 87° 36′ E), which is near AKD (Fig. 8).

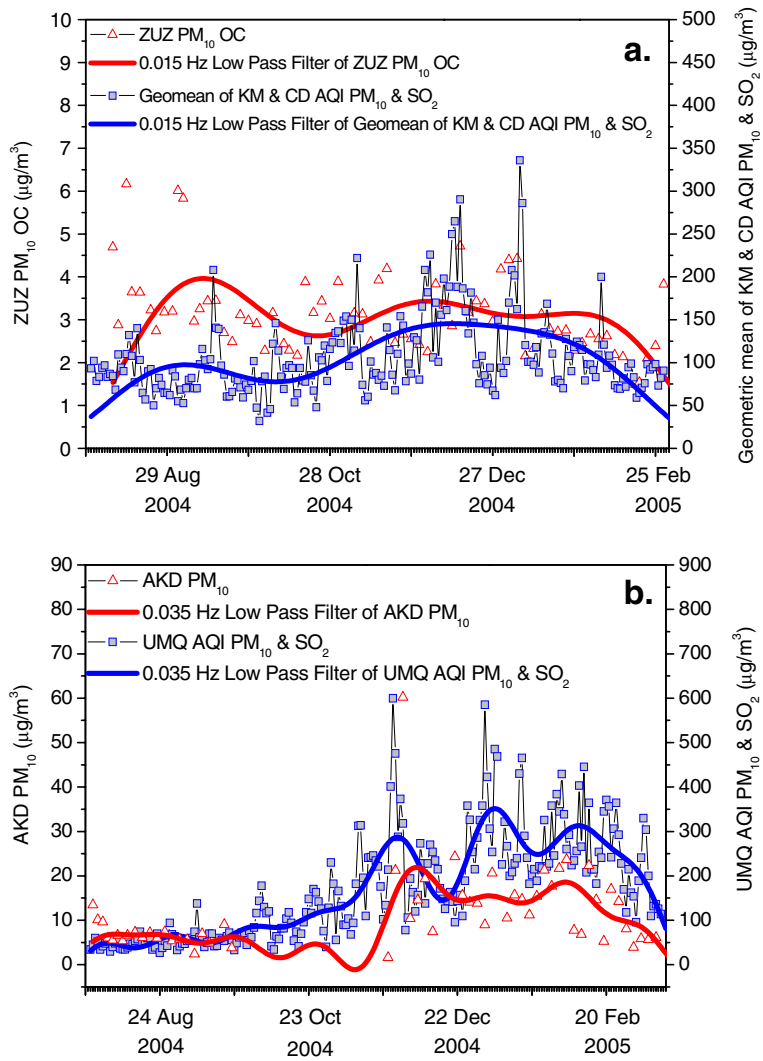

Fig. 8 Comparison of the measured PM_{10} organic carbon (*OC*) concentration at Zhuzhang (*ZUZ*) with daily PM_{10} and SO_2 loads deduced from the ground air quality index (*AQI*) in the regional cities of Kunming (*KM*, ~500 km distant) and Chengdu (*CD*, ~570 km distant; **a**); comparison of measured PM_{10} concentration at Akdala (*AKD*) with daily PM_{10} and SO_2 loads deduced from the ground AQI in the regional city of Urumqi (*UMQ*, ~530 km distant; **b**)

The daily PM_{10} loads of the regional cities were deduced from the ground air quality index (AQI; State Environmental Protection Administration, available at http://www.sepa.gov.cn/quality/air.php3) for most of the days for which PM_{10} was reported as the principal pollutant. Based on the technological rules related to AQI, the following formula was used to derive the PM_{10} concentration from AQI:

$$C = \left[(I - I_{\text{low}})/(I_{\text{high}} - I_{\text{low}})\right] \times (C_{\text{high}} - C_{\text{low}}) + C_{\text{low}}, \quad (1)$$

where C is the concentration of PM_{10}, I_{low} and I_{high} are AQI grading limited values that are lower and larger than I (AQI index), respectively, and C_{high} and C_{low} denote the PM_{10} concentrations corresponding to I_{high} and I_{low}, respectively. The daily SO_2 loads were also deduced in the same manner as used to deduce the PM_{10} for several days, during which SO_2 was reported as the principal pollutant. The deduced daily PM_{10} and SO_2 loads were subsequently merged into a continuous time series.

The concentrations of aerosol populations observed at AKD were directly compared with the deduced daily PM_{10} and SO_2 loads in UMQ. However, for ZUZ, the major transport pathways for air pollutants came from Sichuan Basin (C-3) where CD situated and from southeastern Yunnan Province (C-2) where KM situated (Fig. 1, Table 1). Therefore, records in KM and CD were used to calculate the daily geometric mean PM_{10} and SO_2 loads, which were subsequently compared to the results observed at ZUZ.

The measured PM_{10} OC concentration at ZUZ showed variation trends similar to the geometric mean time series of the deduced daily PM_{10} and SO_2 loads for KM and CD (Fig. 8a). The measured PM_{10} concentrations at AKD also covaried with the deduced daily PM_{10} and SO_2 loads for UMQ (Fig. 8b). Linear regressions between data from our monitoring sites (ZUZ and AKD) and the daily PM_{10} and SO_2 loads deduced from the ground AQI in the regional cities (~500 km distant) yielded correlation coefficients (r) ranging from 0.39 to 0.68 ($p < 0.01$ significance). These comparisons revealed that the aerosols observed at ZUZ and AKD can reflect variation of the regional pollutants.

Comparison of OC/EC concentrations at ZUZ and AKD with other background sites

The observed OC concentrations in PM_{10} at ZUZ and AKD (arithmetic mean ± standard deviation, 3.1 ± 0.91 and 2.9 ± 1.6 μg m^{-3}) were comparable with those of other background sites in South Korea, America and Hungary (Table 2). In addition, these values also were similar to the OC background level in America (~3 μg m^{-3}; Malm et al. 1994) and comparable with OC concentrations in the boundary layer (median of 5.8 μg m^{-3}) and the free troposphere (median of 3.9 μg m^{-3}) over the North Pacific (Huebert et al. 2004). Similarly, the EC concentrations at ZUZ and AKD (0.34 ± 0.18 and 0.35 ± 0.31 μg m^{-3}, respectively) were comparable to the above-mentioned background sites and Mt. Waliguan in China. However, Lim et al. (2003) reported lower EC concentrations of 0.09 μg m^{-3} over the background Pacific Ocean. Moreover, the OC and EC concentrations at Lin'an regional background site were much higher than those at ZUZ and AKD. Lin'an is in Zhejiang Province, which is a heavily populated area in southeastern China that is subject to strong anthropogenic emissions.

It is worth noting that there are high OC and EC levels at urban sites in India, Pakistan, and Bengal (Table 2). As important source regions of air parcels transported to ZUZ, the impact of carbonaceous aerosol emission from these neighboring countries to southwestern China requires further investigation.

Discussion

Inter-relationships and possible sources of the aerosol populations at ZUZ and AKD

Aerosol ions and trace elements at ZUZ

Sea salt Ionic Na^+ was generally the second most abundant WS ion following SO_4^{2-} in ZUZ PM_{10} samples during the course of study. Na^+ is

Table 2 Comparison of organic carbon (OC) and elemental carbon (EC) concentrations at Zhuzhang (ZUZ) and Akdala (AKD) with the results from other background sites

Location	Period	Concentration ($\mu g\ m^{-3}$)		Size	Sites property	References
		OC	EC			
Zhuzhang, Yunnan, China	Aug, 2004	3.7 ± 1.0[a]	0.45 ± 0.25	PM_{10}	Regional background site	This study
	Autumn, 2004	3.2 ± 0.88	0.30 ± 0.16			
	Winter, 2004	2.9 ± 0.82	0.36 ± 0.17			
	Aug, 2004–Feb, 2005	3.1 ± 0.91	0.34 ± 0.18			
Akdala, Xinjiang, China	Aug, 2004	2.5 ± 0.83	0.19 ± 0.07	PM_{10}	Regional background site	This study
	Autumn, 2004	2.5 ± 1.3	0.25 ± 0.31			
	Winter, 2004	3.3 ± 1.8	0.45 ± 0.32			
	Aug, 2004–Feb, 2005	2.9 ± 1.6	0.35 ± 0.31			
Lin'an, Zhejiang, China	Nov, 1999	42∼44	3.0∼3.4	$PM_{2.5}$	Regional background site	Xu et al. (2002)
	Feb–Apr, 2001		2.5	$PM_{2.5}$		Wang et al. (2004)
Waliguan, Qinghai, China	Jul, 1994–Dec, 1995		0.13∼0.3		Global background site	Tang et al. (1999)
Kosan, South Korea	Apr, 1999	2.8 ± 0.20	0.09 ± 0.01	$PM_{2.5}$	Background site	Kim et al. (2000)
Kangwha, South Korea	Apr, 1999	4.8 ± 0.79	0.26 ± 0.06	$PM_{2.5}$	Background site	Kim et al. (2000)
Look Rock, Tennessee, America	2001	1.9∼4.0	0.55∼0.65	$PM_{2.5}$	Background site	Tanner et al. (2004)
Budapest, Hungary	Apr–May, 2002	2.9∼5.5	0.19∼0.64	$PM_{2.0}$	Background site	Salma et al. (2004)
Mumbai, India	Mar, 1999	25.3	12.6	PM_{10}	Urban site	Venkataraman et al. (2002)
Lahore, Pakistan	Sep, 1992–Sep, 1993	76.9	17.6	TSP	Urban site	Smith et al. (1996)
Dhaka, Bangladesh	Apr–May, 2001	45.7	22.0	TSP	Urban site	Salam et al. (2003)

[a] Arithmetic mean ± standard deviation

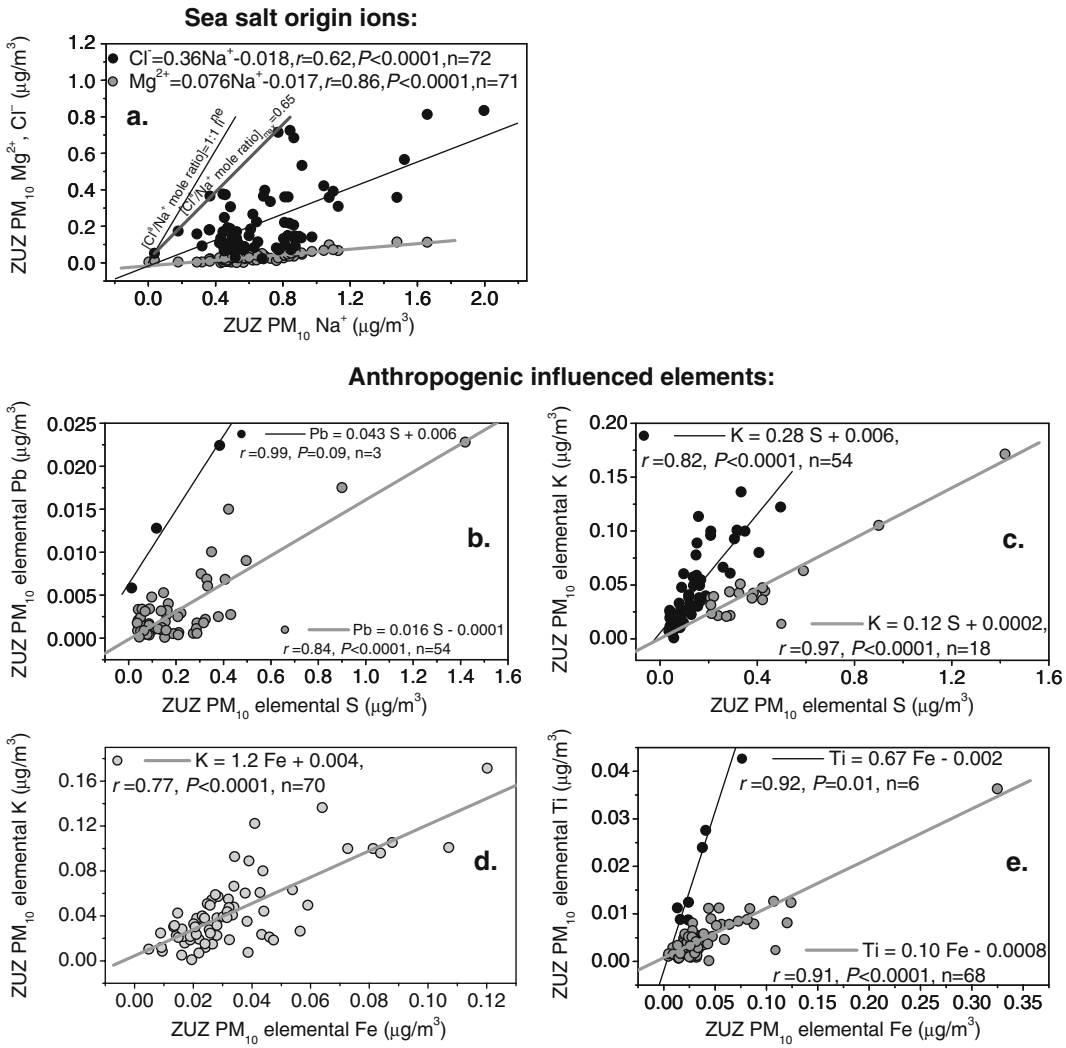

Fig. 9 Linear correlations of *sea salt origin ions* (**a**) between ionic Cl^-, Mg^{2+}, and Na^+ in PM_{10} at Zhuzhang (*ZUZ*); linear correlations of *anthropogenic influenced elements* between elemental Pb and S (**b**), between K and S (**c**), between anthropogenic influenced K and crust origin Fe (**d**), and between Ti and crust origin Fe (**e**) in PM_{10} at ZUZ

commonly used as an indicator of sea salt (Arimoto et al. 2004; Piel et al. 2006). The close relationships between Na^+ and Mg^{2+}, Cl^- (Fig. 9a) observed in the present study suggested that there were important marine sources of these ions. These findings were also supported by the high proportion (48.2%) of the trajectories from the Arabian Sea (C-5) and from coastal regions near the Bay of Bengal (C-1 and C-4; Fig. 1, Table 1). The prevailing southwest monsoon is advantageous to sea salt aerosol input by maritime air parcels. The highest concentrations of WS Na^+, Mg^{2+}, and Cl^- were observed in samples from the remote southwesterly trajectories from the Arabian Sea (C-5; Qu et al. 2008), which is consistent with their sea salt origin.

The Cl^-/Na^+ ratio determined from linear regression (mass concentration ratio=0.36) deviates from the Cl^-/Na^+ mole ratio = 1:1 line (Fig. 9a), which suggests that there is a Cl^- deficit due to chemical evolution of the marine source aerosols during transport. However, the maximum Cl^-/Na^+ mole concentration ratio (0.65) could approach 1 under specific meteorology.

Crust origin and anthropogenic influenced material Six major elements in the ZUZ PM_{10} samples, including Ca, Fe, Ti, Si, Al, and Mg, exhibited synchronous variations and significant inter-correlations ($p < 0.01$ significance, r ranged from 0.45 to 0.70, $n = 74$). Their EF_{crust} values were less than 5, indicating that they were typically associated with crustal material. Similarly, elemental Mn and Sr were also primarily of crust origin.

Conversely, significant correlations ($p < 0.05$ significance, r ranged from 0.29 to 0.96, $n = 30$–59) were also identified among Zn, Zr, Pb, As, Ni, Se, V, Cu, Cr, and P, but their EF_{crust} values were significantly larger than 5, which suggests that they were influenced by non-crustal, anthropogenic sources. In addition, the Pb/S ratio for most of the samples ($n = 54$) was 0.016, but it was 0.043 for three other samples (Fig. 9b); the latter samples may reflect contribution of the major polluted C-3 trajectories (Fig. 1, Table 1), which accounted for 3.9% of the total trajectories and had the highest Pb concentration (Qu et al. 2008).

Linear regression indicated that the K/S ratio was 0.28 for most of the ZUZ PM_{10} samples ($n = 54$), but it was only 0.12 for another group of samples ($n = 18$, Fig. 9c); the higher value of the former samples was likely due to biomass burning. In addition, there was a higher K/Fe ratio for the ZUZ PM_{10} samples (1.2, Fig. 9d) when compared with the same ratio of the crust (0.8, Taylor and McLennan 1995), which indicates that K was influenced by anthropogenic sources (e.g., biomass burning). The Ti/Fe ratio for most of the samples ($n = 68$) was 0.10 (Fig. 9e), which was similar to that of the crust (0.09, Taylor and McLennan 1995); these results suggest that Ti primarily originated from crustal material. However, six samples had a higher Ti/Fe ratio (0.67, Fig. 9e) than the crust, which indicates that they may have been influenced by industrial emissions such as those from the Sichuan Basin.

Aerosol ions and trace elements at AKD

Soil dust Good correlations were identified among Ca^{2+}, Mg^{2+}, and Na^{+} in the AKD PM_{10} samples (Fig. 10a and b). The TSP samples also showed good correlations between Mg^{2+} and Na^{+} (Fig. 10c) and significant correlations ($p < 0.01$ significance) between NO_3^- and Ca^{+} ($r = 0.75$, $n = 22$). There were also significant correlations between Cl^- and Na^{+} in both PM_{10} and TSP (Fig. 10d). Moreover, in the TSP, these ions (typically represented by Mg^{2+} and Ca^{+}) were also significantly correlated with the presumed crustal origin elements such as Ca, Fe, Ti, and Mn (r ranged from 0.54 to 0.78, $n = 22$). Taken together, these findings indicate that the aforementioned ions may originate from or be influenced by WS salts in the salinized soil and crustal material.

AKD is located in inland Eurasia; the land covers around and in the neighborhood (including Xinjiang, most of Mongolia and the neighboring areas in Russia and Kazakhstan) were the arid Gobi and desert. Therefore, the WS salts that accumulated in the surface salinized soil from such land covers were likely entrained into the atmosphere by the strong surface winds, after which they could be transported to our study site and became important source of aerosol ions. Year-round arid climate and intensive wind may lead to the constant contribution of the WS salts (from the soil) to the aerosol ions. With the exception of three samples collected during dust events on Nov 30th 2004 and Jan 2nd and Jan 5th 2005, consistent relationships among Ca^{2+}, Mg^{2+}, Na^{+}, and SO_4^{2-} were observed for the PM_{10} samples ($n = 54$; Fig. 10a, b, e, and f), which supports this contention. Information regarding transport supplies more evidence. The westerly trajectories to AKD (C–B, C–C, C–D, and C–E, accounting for 70% of the total trajectories; Fig. 1, Table 1) exhibited comparatively high levels of Ca^{2+} and Mg^{2+}, as well as quite similar concentrations of Na^{+} (Qu et al. 2008). These properties may reflect salinized dust delivered by the prevailing winds from sandy lands and deserts in eastern Kazakhstan and in the area.

Other studies also have reported that aerosol ions originated from the salinized soil. Chemical analysis and surface structure analysis of the individual particles have shown that the aerosol Na^{+}, Cl^-, and SO_4^{2-} during dust storms in Beijing most likely originated from the salinized soil that was enriched with chloride and sulfate (Zhang et al. 2004). Comparison of dust from the source

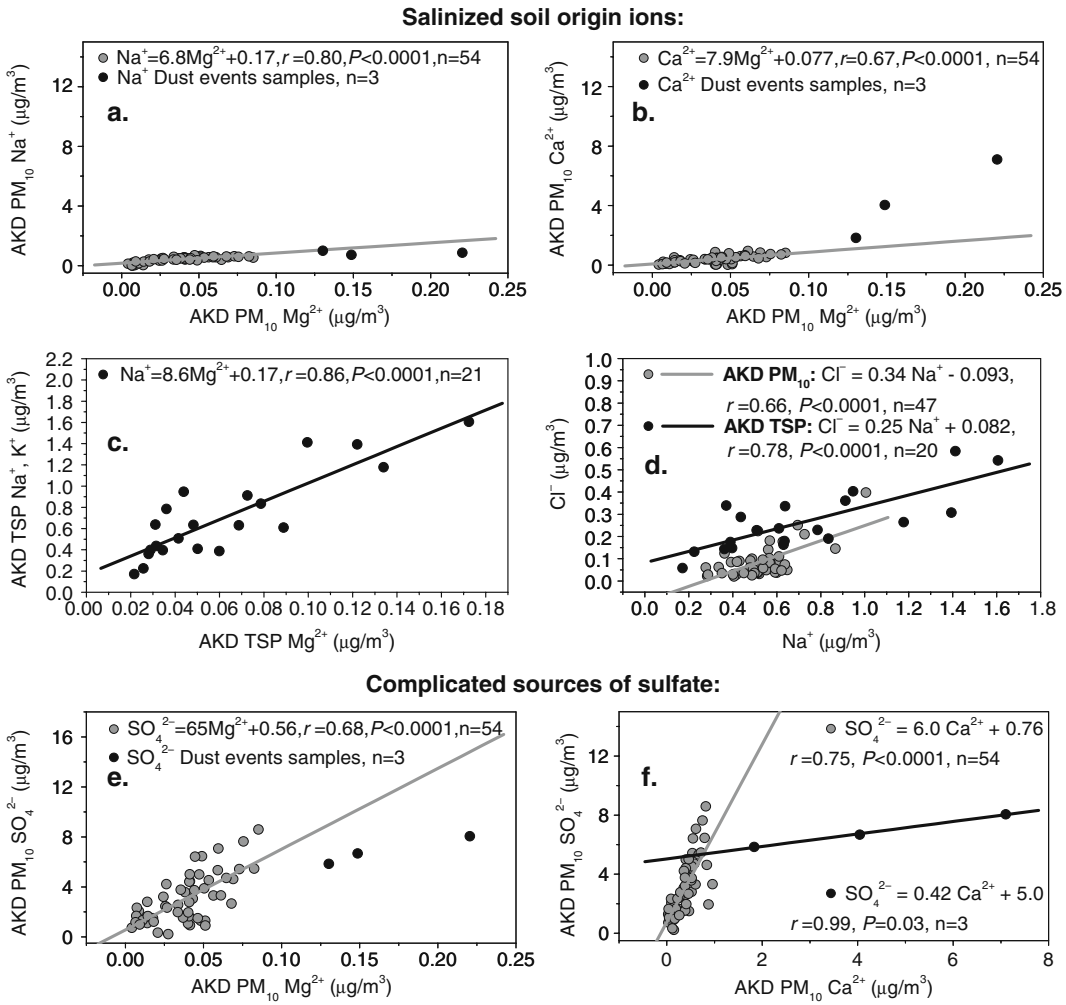

Fig. 10 Linear correlations of *salinized soil origin ions* between ionic Na^+ and Mg^{2+} (**a**), between Ca^{2+} and Mg^{2+} (**b**) in PM_{10}, between Na^+ and Mg^{2+} in TSP (**c**), and between Cl^- and Na^+ in PM_{10} and TSP (**d**) at Akdala (*AKD*). Linear correlations of *sulfate* between ionic SO_4^{2-} and Mg^{2+} (**e**) and between SO_4^{2-} and Ca^{2+} (**f**) in PM_{10} at AKD

region and the deposition region has revealed that the peak concentrations of Ca^{2+}, SO_4^{2-}, Cl^-, and Na^+ in particles larger than 3.3 μm originated from WS salts in the soil dust (Liu et al. 2003). Furthermore, evaluation of aerosols from the Taklimakan Desert has revealed a local soil origin of the crustal elements from salts accumulated in the surface (Makra et al. 2002).

At AKD, elemental Al, Fe, Ca, K, Ti, Mn, and Sr in the PM_{10} and Fe, K, Ca, Ti, Mn, and Se in the TSP were found to be closely related, as indicated by correlation coefficients of linear regressions (r) ranging from 0.92 to 0.99 ($p < 0.05$ significance). The strong correlations between these elements with Ca and Fe (typical crustal origin elements, Zhang et al. 2003) indicated that they most likely originated from crustal material. Elemental Se also showed strong correlations with these presumed crustal elements (r ranged from 0.96 to 0.98, $n = 15$, $p < 0.01$ significance) in TSP. In addition, EF_{crust} values for these elements (Ca, Fe, K, Ti, Al, Mn, Sr, Si, and Mg) were all close to unity (maxima less than 5), which is consistent with their crustal origin.

Complicated source of sulfate It is worth noting that the origin of SO_4^{2-} at AKD was likely complicated, including both a crustal source and anthropogenic influence. Good correlations were observed among Ca^{2+}, Mg^{2+}, and SO_4^{2-} in most of the AKD PM_{10} samples ($n = 54$, Fig. 10e and f). Moreover, ionic SO_4^{2-} in the TSP was significantly correlated with the presumed crustal origin elements such as Ca, Fe, Ti, and Mn (r ranged from 0.61 to 0.63, $n = 22$). These results suggest a crustal source of SO_4^{2-} from WS salts in the surface salinized soil. Along this same line, the SO_4^{2-}/WS Ca^{2+} mole concentration ratio for the three PM_{10} samples collected during dust events (0.18, corresponding to a mass concentration ratio of 0.42, Fig. 10f) was comparable to those of the dust storm samples in the Mu Us Desert (0.1, Arimoto et al. 2004). However, the SO_4^{2-}/WS Ca^{2+} mass concentration ratio (= 6.0) for most of the samples ($n = 54$) was approximately 14 times the ratio of samples collected during the three dust events (Fig. 10f), indicating that anthropogenic sources such as coal combustion likely contributed to the ionic SO_4^{2-} in PM_{10} at AKD for most of the sampling days. The results from a subsequent source apportion with PCA ("Source apportion of the aerosols at ZUZ and AKD") also support this contention, that is, SO_4^{2-} had a high loading on an anthropogenic component as well as a moderately high loading on a soil dust component. Ionic NO_3^- showed similar consistency, which indicates that it was substantially loaded on a soil dust component and moderately loaded on an anthropogenic component.

There are two possible causes of the good intercorrelation between ionic SO_4^{2-} and NO_3^- with ions of crustal origin such as Ca^{2+}: (1) they originated from the same source, such as the salinized soil dust; (2) SO_4^{2-} was associated with dust particles due to uptaking of SO_2 by the dust particles through heterogeneous reactions during their mixing and transport to the site. These processes involved external mixing of various types of pollutants and particles, as well as their internal mixing (such as chemical uptake of SO_2 and HNO_3 by the dust particles). The internal mixing may result in coexistence of the aerosol populations from different sources in the aged aerosol. It is difficult to determine the detailed mechanism of the good inter-correlation between SO_4^{2-} and ions of crustal origin (e.g., Ca^{2+}) based our data alone. Nevertheless, the larger SO_4^{2-}/Ca^{2+} ratio observed for most of our samples compared with the dust storm samples in the Mu Us Desert tends to support the latter inference. Further investigation, such as comparing the ionic composition of aerosol samples and salinized soil dust samples from around the region, should be conducted to gain a better understanding of this phenomenon.

Anthropogenic influenced material When elemental S, Cu, Zn, Ni, and As were evaluated, good correlations were observed between S and OC, NH_4^+, and SO_4^{2-} ($r = 0.92$, 0.97 and 0.75, $n =$ 8, 14, and 17, respectively, $p < 0.01$ significance), between S and Cu and Zn ($r = 0.93$ and 0.86, respectively, $n = 17$, $p < 0.0001$ significance), and between Zn and Cu and Ni ($r = 0.92$, $n = 17$, $p < 0.0001$ significance) in PM_{10} at AKD. In addition, the EF_{crust} values for Zn, Pb, As, Ni, Cu, and Cr (larger than 5) indicated influences from non-crustal sources. Taken together, these results indicate that these elements may have a close origin and represent regional industrial emissions. Trajectories that originated at or passed over the regional industrial and mining areas (C–J, C–G, and C–A) were likely the major pathways for pollutant transport to AKD (Fig. 1, Table 1). There were also significant correlations ($p < 0.05$ significance, r ranged from 0.68 to 0.97, $n = 9$–22) between elemental Pb, Cu, Zn, As, Ni, and V in the TSP at AKD, which is consistent with their anthropogenic origin likely being from regional industries.

Source apportion of the aerosols at ZUZ and AKD

In a further attempt, PCA with VARIMAX normalized rotation was applied to the aerosol chemical composition data at the two sites to assist in identification of the possible sources of pollutants. Table 3 displays the factor loadings obtained using the VARIMAX rotation, as well as the eigenvalues.

PCA identified three components at ZUZ that explained 72.4% of the total variance in the aerosol data set. PC1 was highly loaded with SO_4^{2-}

Table 3 Varimax orthogonal rotated principal component matrix for organic carbon (OC), elemental carbon (EC), and water-soluble ionic species in PM_{10} aerosol at Zhuzhang (ZUZ) and Akdala (AKD)

Aerosol species and parameter	Component 1	2	3	4	Communalities
Zhuzhang (ZUZ)					
OC	0.26	***0.81***	0.14		0.75
EC	***0.55***	***0.73***	−0.14		0.86
OC/EC	**−0.42**	**−0.38**	***0.64***		0.73
Na^+	0.24	**0.34**	***0.83***		0.86
NH_4^+	***0.88***	−0.09	−0.19		0.82
K^+	***0.81***	0.11	**0.37**		0.81
Mg^{2+}	**0.49**	0.10	***0.72***		0.77
Ca^{2+}	−0.09	***0.69***	**0.38**		0.64
Cl^-	−0.04	0.29	***0.70***		0.58
SO_4^{2-}	***0.81***	0.16	0.15		0.71
NO_3^-	−0.07	***0.65***	0.12		0.45
Initial eigenvalue	4.10	2.27	1.59		
Percent of variance	**26.9**	**22.8**	**22.7**		
Cumulative percent	26.9	49.7	72.4		
Likely source	Fuel combustion (coal, biomass, etc.)	Dust/pollutant mixed	Sea salt		
Akdala (AKD)					
OC	***0.51***	−0.01	0.22	***0.83***	0.99
EC	***0.85***	0.03	**0.39**	0.07	0.89
OC/EC	**−0.37**	−0.05	−0.19	***0.89***	0.96
Na^+	0.13	***0.57***	***0.71***	0.01	0.84
NH_4^+	***0.81***	**0.46**	−0.07	−0.13	0.90
K^+	***0.80***	0.01	**0.43**	0.05	0.83
Mg^{2+}	0.26	***0.86***	**0.38**	−0.06	0.96
Ca^{2+}	0.11	***0.93***	0.17	−0.01	0.90
Cl^-	0.12	0.24	***0.87***	0.03	0.84
SO_4^{2-}	***0.83***	***0.51***	0.04	−0.07	0.96
NO_3^-	**0.48**	0.11	***0.64***	−0.12	0.67
Initial eigenvalue	5.47	1.68	1.45	1.11	
Percent of variance	**31.4**	**22.4**	**20.7**	**13.8**	
Cumulative percent	31.4	53.8	74.5	88.3	
Likely source	Fuel combustion (coal, biomass, etc.)	Soil dust	Salinized soil dust	Semi-volatile and secondary organic carbon	

PCA loadings greater than ±0.3 are shown in bold, and those greater than ±0.5 are shown in bold italics

(0.81), NH_4^+ (0.88), and K^+ (0.81), as well as moderately loaded EC (0.55). These results indicate that PC1 represented an anthropogenic source of pollutants from fuel combustion (coal, biomass, etc.). PC2 was highly loaded with OC (0.81) and EC (0.73), as well as NO_3^- (0.65) and Ca^{2+} (0.69), which indicates that it represented a mixture of anthropogenic pollutants and dust. The OC/EC ratios were negatively correlated with PC1 and PC2 (loadings = −0.42 and −0.38, respectively), which was likely due to the generally low OC/EC ratio of the primary carbonaceous aerosols from anthropogenic emissions. Na^+, Mg^{2+}, and Cl^- were highly loaded (loadings = 0.83, 0.72, and 0.70, respectively) on PC3, which indicates that it was a sea salt component. This source was likely associated with maritime air parcels transport from the Bay of Bengal and the Arabian Sea

(Fig. 1, Table 1), during which accompanied with formation of secondary OC and diffusion/dilution of EC; these processes may result in the increased OC/EC ratio and its positive correlation with PC3 (loadings = 0.64).

When the aerosol data set at AKD was considered, PCA revealed four components accounting for 88.3% of the total variance. PC1 was characterized by EC (loading = 0.85), SO_4^{2-} (0.83), NH_4^+ (0.81), and K^+ (0.81), while OC loading (0.51) was also moderately high on this component. These results indicate that PC1 was a typical anthropogenic source of fuel combustion (coal, biomass, etc.). As discussed above, the OC/EC ratio was negatively correlated with this component. PC2 and PC3 were both ascribed to soil dust sources; however, PC2 was characterized by high Ca^{2+} (0.93) and Mg^{2+} (0.86) loadings as well as moderately high Na^+ (0.57) and SO_4^{2-} (0.51) loadings, while PC3 was characterized by high Cl^- (0.87) and Na^+ (0.71) loadings as well as substantially high NO_3^- loading (0.64). These results indicate that PC3 may reflect a typical salinized soil dust source from the arid Gobi, desert, or similar land covers in and around the region. The last component (PC4) was only highly loaded with OC (0.83), and the OC/EC ratio was strongly positively correlated (loading = 0.89) with this component. These results indicate that PC4 may reflect the natural SVOC (with no EC emission accompanied) and SOC formed during regional transport to this remote site.

Regional representativeness of the ZUZ and AKD sites

The results of this study indicate that the aerosols collected at both ZUZ and AKD were regionally representative, which was supported by five factors:

1. *The locations of the sites*: Both ZUZ and AKD are remote rural sites situated at high altitudes; therefore, the aerosols collected were likely primarily delivered by regional or distant transport with limited impacts from local circulation and anthropogenic emissions.
2. *The well-mixed state of the atmosphere*: Covariation between the aerosol populations that appeared to be from different sources and constant EC (a typical primary pollutant) contributions to the aerosol mass (5.1% at ZUZ versus 3.5% at AKD) implied that the atmosphere sampled was likely well-mixed.
3. *The geographical coverage of regional transport*: Measurements at ZUZ may represent regional atmosphere conditions in southwestern China including Yunnan, Sichuan, Guizhou, Chongqing, and Tibet, in which the transport pathways passed over (Fig. 1, Table 1). Measurements at ZUZ may also reflect the influences of pollutant input from South Asian countries such as India, Burma, Bangladesh, and Nepal. The results at AKD can arguably reflect the atmosphere conditions in northern Xinjiang Province and neighboring areas through which the transport pathways passed, with also influences of pollutants from upwind countries.
4. *The comparable aerosol levels with other background sites*: The observed OC and EC concentrations at ZUZ and AKD were comparable to other background sites, indicating that baseline aerosol characteristic could be obtained at both sites.
5. *The covariation trend of the observed aerosols in comparison with regional cities*: The measured aerosol species at both sites varied synchronously with the PM_{10} and SO_2 loads in the regional cities, indicating that observation at ZUZ and AKD can reflect the variation and regularity of the regional atmospheric composition.

Therefore, aerosols collected at ZUZ and AKD can be expected to be reasonable representations of the regionally well-mixed atmosphere and a potentially suitable reference for analysis of regional atmospheric backgrounds.

However, with the change in seasons, the representative regions (typically the upwind sectors) of these background sites varied because of changes in atmospheric transport. Indeed, the source areas, directions, transport distances, and coverage areas of the individual backward trajectories to

ZUZ and AKD differed greatly during different seasons. For example, the transport pathways to ZUZ (Fig. 1, Table 1) during August (late summer) were primarily short, including the southwesterly trajectories from coastal countries near the Bay of Bengal (C-1 and C-4, accounted for 44% of all trajectories), the southeasterly trajectories from over southeastern Yunnan Province and south Asian countries (C-2, 38%), and the northeasterly trajectories from the Sichuan Basin and beyond (C-3, 18%). However, during autumn, winter, and early spring, the pattern of transport differed greatly and included more remote trajectories from the west (West Asia, C-6), northwest (East Europe, C-7) and southwest (Arabian Sea, C-5); specifically, the proportion of these trajectories increased to 28% and 72% during autumn and winter, respectively. Other features of wintertime transport to ZUZ were south-westward migration and extension of the coverage area of the major individual trajectories as well as the absence of the northeasterly trajectories. At AKD, geographical distributions of the trajectories (Fig. 1, Table 1) were generally similar in different seasons. However, there were more trajectories from the northern high latitudes during mid–late summer and autumn, more southeasterly trajectories from over the boundary area between northwestern China and Mongolia during early spring (C–A, 17% of all trajectories), and southward migration of the coverage area of the major individual trajectories during winter. The variation in atmospheric transport resulted in seasonality of the representative regions and scales of these sites, which needs further assessment.

Further quantitative study is necessary to assess the regional representativeness of these two background sites. Such studies (similar to the study conducted by Blanchard et al. (1999) in San Joaquin Valley) should include an estimation of the scale of transport based on the observation from multisites in these regions.

OC/EC ratio used as a means of distinguishing polluted periods

Because of the inevitable occurrence of disturbances from natural emissions, anthropogenic activities, and regional input, identification of the data with the least perturbation is essential for determining aerosol background levels. Hidy and Blanchard (2005) reported that median values for the lower parts of the concentration distributions, as well as the variation and frequency of these values derived from long-term and multisite observations, provide a better representation of background conditions. We also have suggested using the OC/EC ratio as a means of distinguishing polluted periods from background conditions combined with examining the statistic distribution and variation of the data to estimate aerosol background concentrations at ZUZ and AKD (Qu et al. 2009). This approach is based on the fact that the OC/EC ratio can increase during transport as a result of secondary transformed SOC being added to the primary OC fraction, while the OC/EC ratio for the proximate primary sources was most likely smaller. The lower OC/EC ratio group of samples may reflect influences from proximate sources; for example, the aerosol populations (including OC, EC, SO_4^{2-}, NO_3^-, and soil dust) from lower OC/EC ratio samples at both ZUZ and AKD generally exhibited higher levels and larger variabilities when compared with the group of samples with higher OC/EC ratio (Qu et al. 2009). Conversely, the higher OC/EC ratio group can be expected to represent a well-mixed atmosphere delivered by regional or distant transport with signatures of the regional background.

Indeed, the concentrations of SO_4^{2-} (a major aerosol component at both sites, Qu et al. 2008) and the sum of OC + EC + ions exhibited reasonable first-order exponential-decay fitting with the OC/EC ratios at both sites (Fig. 11), similar to the fitting of EC concentrations with OC/EC ratios (Qu et al. 2009). These fitting curves reveal that, as the concentrations of EC, SO_4^{2-}, and the sum of OC + EC + ions increased, the OC/EC ratios approached a constant value that may represent the characteristic OC/EC ratio of the proximate primary emission sources; while as the OC/EC ratios increased, the concentrations of EC, SO_4^{2-}, and the sum of OC + EC + ions approached low values, which might reflect their background levels. Moreover, SOC/(OC + EC + ions) was found to be significantly correlated with the OC/EC ratio (Fig. 11), which also indicates that as the SOC proportion increases, the OC/EC ratio increases.

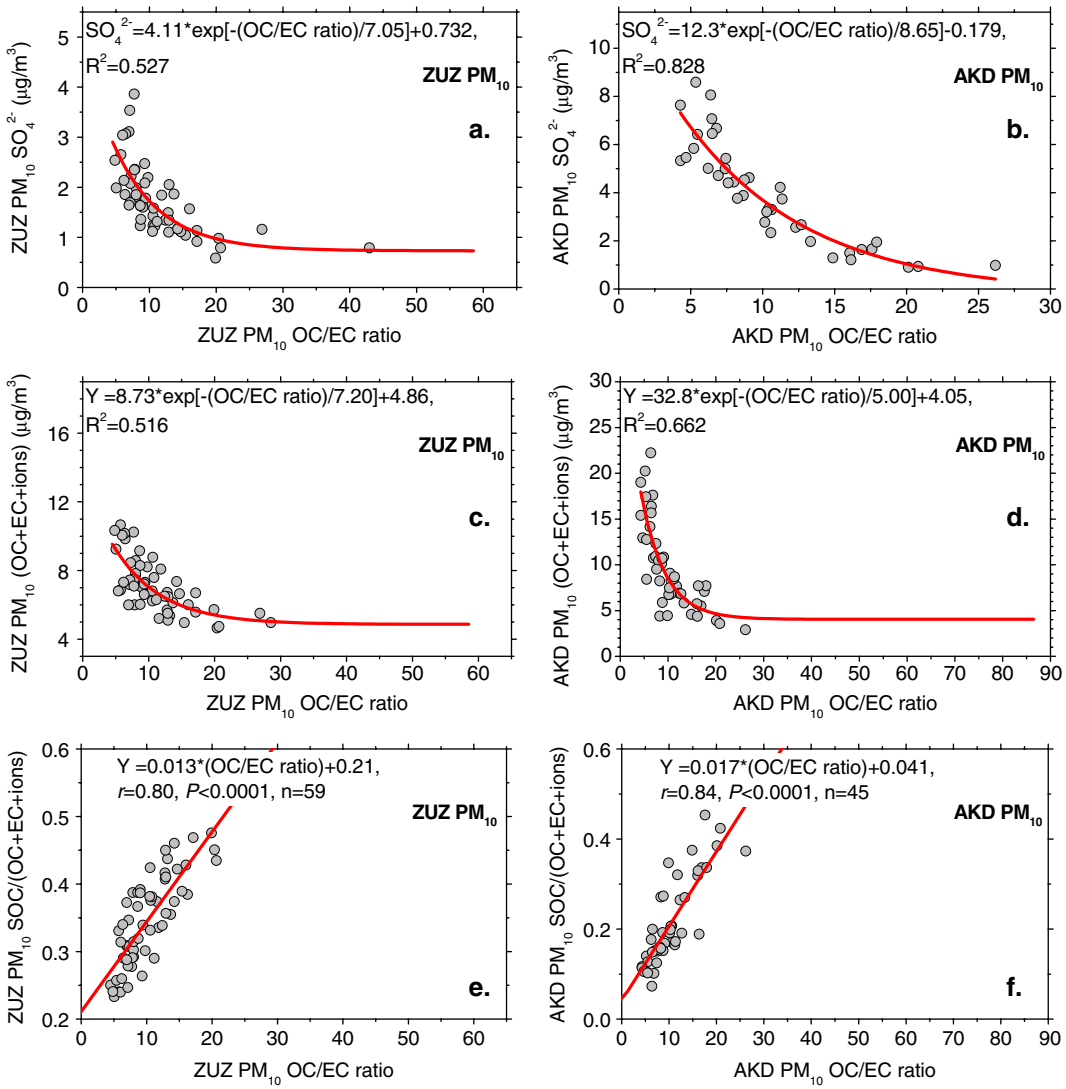

Fig. 11 First-order exponential-decay fitting between PM_{10} OC/EC ratio and SO_4^{2-} concentration at ZUZ (**a**) and AKD (**b**) indicates variation trend of sulfate with OC/EC ratio; first-order exponential-decay fitting between PM_{10} OC/EC ratio and Sum (OC + EC + ions) concentration at ZUZ (**c**) and AKD (**d**) indicates variation trend of Sum (OC + EC + ions) concentration with OC/EC ratio; linear regression fitting between PM_{10} OC/EC ratio and SOC/Sum (OC + EC + ions) at ZUZ (**e**) and AKD (**f**) indicates SOC contribution increases as OC/EC ratio increases

The relationship between variation in the aerosol populations and the OC/EC ratio indicate that it may be feasible to use the OC/EC ratio to distinguish samples from regional transport from those that have been influenced by proximate emissions, which is helpful for regional atmospheric background assessment. However, further investigation of the general applicability of this approach for evaluating pollution levels at other remote sites is necessary.

Summary

As part of the evaluation of the two recently planned CAWANET observatory stations (ZUZ

and AKD) in southwestern and northwestern China, aerosol measurements were made to assess the regional representativeness of the two sites. Seasonal variations and the sources of the aerosol species were also investigated.

1. Our study suggested that the ionic Ca^{2+}, Mg^{2+}, Na^{+}, and Cl^{-} in the PM_{10} and TSP at AKD had a crustal origin. Microscopic evaluation of the individual particles may provide morphological evidence in a future study. Additionally, significant correlations between SO_4^{2-}, K^{+}, and EC in the PM_{10} and between EC and elemental S in the TSP revealed contributions from coal combustion and biomass burning. The SO_4^{2-} to WS Ca^{2+} ratio indicated that an anthropogenic source contributed to SO_4^{2-} on most of the sampling days. Moreover, comparison of the PM_{10} and TSP at AKD implied that crust origin ions like Ca^{2+}, Mg^{2+}, and Na^{+} were likely enriched in the TSP, whereas the SO_4^{2-} and K^{+} in the PM_{10} accounted for 72% and 94% of those in the TSP, respectively, confirming the influence of anthropogenic sources.
2. Trace elements in the aerosol were categorized into two sources at both sites, elements with typical crustal origins such as Al, Ca, Fe, Ti, and Si, which showed significant intercorrelations with EF_{crust} values less than 5, and Pb, As, Zn, Ni, V, Cr, and Cu with EF_{crust} values greater than 5, which suggested influences from non-crustal, likely anthropogenic sources.
3. At ZUZ, three main source types were defined based on PCA (in parentheses are the aerosol species characteristic for each source type). These were (a) anthropogenic emissions from fuel combustion such as coal, biomass, etc. (SO_4^{2-}, NH_4^{+}, K^{+}, and EC); (b) mixtures of anthropogenic pollutants and dust (OC, EC, NO_3^{-}, and Ca^{2+}); and (c) sea salt (Na^{+}, Mg^{2+}, and Cl^{-}). These components explained 26.9%, 22.8%, and 22.7% of the total variance of the data set, respectively. At AKD, four main source types were identified: (a) anthropogenic fuel combustion (EC, SO_4^{2-}, NH_4^{+}, K^{+}, and OC); (b) soil dust (Ca^{2+}, Mg^{2+}, Na^{+}, and SO_4^{2-}); (c) salinized soil dust (Cl^{-}, Na^{+}, and NO_3^{-}); (d) semi-volatile organic carbon and secondary organic carbon (high loadings of OC and a high OC/EC ratio). These components explained 31.4%, 22.4%, 20.7%, and 13.8% of the total variance, respectively.
4. Based on the locations of the sites, well-mixed state of the atmosphere, geographical coverage of the regional transport, comparable aerosol levels with other background sites, and the probability of the observed aerosols reflecting the variation of the regional atmospheric composition, we concluded that observations at ZUZ and AKD can reflect the background atmosphere. Furthermore, these sites are also suitable for monitoring the transboundary influx of pollutants due to the many trajectories from abroad.

Finally, it should be noted that $PM_{2.5}$ measurements can better support a study of regional representativeness than PM_{10}. Unfortunately, $PM_{2.5}$ observations were not included in this study, but such measurements will be conducted in the future study.

Acknowledgments We are grateful to both anonymous reviewers for their constructive suggestions and comments. Wenjun Qu acknowledges members of CAWAS at Chinese Academy of Meteorological Sciences for their support and contributions to the project. This work is supported by the National Basic Research Program of China (2006CB403701, 2006CB403702) and the Chinese Ministry of Education's 111 Project (B07036).

References

Arimoto, R., Snow, J. A., Graustein, W. C., Moody, J. L., Ray, B. J., Duce, R. A., et al. (1999). Influences of atmospheric transport pathways on radionuclide activities in aerosol particles from over the North Atlantic. *Journal of Geophysical Research, 104*, 21301–21316.

Arimoto, R., Zhang, X. Y., Huebert, B. J., Kang, C. H., Savoie, D. L., Prospero, J. M., et al. (2004). Chemical composition of atmospheric aerosols from Zhenbeitai, China, and Gosan, South Korea, during ACE-Asia. *Journal of Geophysical Research, 109*, D19S04.

Blanchard, C. L., Carr, E. L., Collins, J. F., Smith, T. B., Lehrman, D. E., & Michaels, H. M. (1999). Spatial representativeness and scales of transport during the

1995 integrated monitoring study in California's San Joaquin Valley. *Atmospheric Environment, 33*, 4775–4786.

Castro, L. M., Pio, C. A., Harrison, R. M., & Smith, D. J. (1999). Carbonaceous aerosol in urban and rural European atmospheres: Estimation of secondary organic carbon concentrations. *Atmospheric Environment, 33*, 2771–2781.

Chow, J. C., Waston, J. G., Pritchett, L. C., Pierson, W. R., Frazier, C. A., & Purcell, R. G. (1993). The DRI thermal/optical reflectance carbon analysis system: Description, evaluation and applications in US air quality studies. *Atmospheric Environment, 27A*, 1185–1201.

Draxler, R. R., & Hess, G. D. (1998). An overview of the HYSPLIT 4 modelling system for trajectories, dispersion, and deposition. *Australian Meteorological Magazine, 47*, 295–308.

Dusek, U. (2000). Secondary organic aerosol—formation mechanisms and source contributions in Europe. Interim Report IR-00-066. Retrieved from http://www.iiasa.ac.at/.

Geron, C., Owen, S., Guenther, A., Greenberg, J., Rasmussen, R., Bai, J. H., et al. (2006). Volatile organic compounds from vegetation in southern Yunnan Province, China: Emission rates and some potential regional implications. *Atmospheric Environment, 40*, 1759–1773.

Hidy, G. M., & Blanchard, C. L. (2005). The midlatitude North American background aerosol and global aerosol variation. *Journal of the Air & Waste Management Association, 55*, 1585–1599.

Huebert, B., Bertram, T., Kline, J., Howell, S., Eatough, D., & Blomquist, B. (2004). Measurements of organic and elemental carbon in Asian outflow during ACE-Asia from the NSF/NCAR C-130. *Journal of Geophysical Research, 109*, D19S11.

Kaiser, H. F. (1960). The application of electronic computers to factor analysis. *Educational and Psychological Measurement, 20*, 141–151.

Kim, Y. P., Moon, K. C., Shim, S. G., Lee, J. H., Kim, J. Y., Fung, K., et al. (2000). Carbonaceous species in fine particles at the background sites in Korea between 1994 and 1999. *Atmospheric Environment, 34*, 5053–5060.

Krivácsy, Z., & Molnár, Á. (1998). Size distribution of ions in atmospheric aerosols. *Atmospheric Research, 46*, 271–291.

Lim, H. J. (2001). Semi-continuous aerosol carbon measurements: Addressing atmospheric progress of local and global concern. Ph.D. thesis, the Graduate School-New Brunswick Rutgers, State University of New Jersey.

Lim, H. J., Turpin, B. J., Russell, L. M., & Bates, T. S. (2003). Organic and elemental carbon measurements during ACE-Asia suggest a longer atmospheric lifetime for elemental carbon. *Environmental Science & Technology, 37*(14), 3055–3061.

Liu, M. Z., Wei, W. S., Zhou, H. F., & Yabuki, S. (2003). Physiochemical properties of atmospheric aerosol particles over sand-dust source areas and sedimentary area in Asia. *Journal of Desert Research, 23*(4), 408–414 (in Chinese).

Loska, K., & Wiechuya, D. (2003). Application of principle component analysis for the estimation of source of heavy metal contamination in surface sediments from the Rybnik Reservoir. *Chemosphere, 51*, 723–733.

Ma, J. Z., Tang, J., Li, S. M., & Jacobson, M. Z. (2003). Size distributions of ionic aerosols measured at Waliguan Observatory: Implication for nitrate gas-to-particle transfer processes in the free troposphere. *Journal of Geophysical Research, 108*(D17). doi:10.1029/2002JD003356.

Makra, L., Borbely, K. I., Koltay, E., & Chen, Y. (2002). Enrichment of desert soil elements in Takla Makan dust aerosol. *Nuclear Instruments and Methods in Physics Research B, 189*, 214–220.

Malm, W. C., Sisler, J. F., Huffman, D., Eldred, R. A., & Cahill, T. A. (1994). Spatial and seasonal trends in particle concentration and optical extinction in the United States. *Journal of Geophysical Research, 99*(D1), 1347–1370.

Moody, J. L., & Galloway, J. N. (1988). Quantifying the relationship between atmospheric transport and the chemical composition of precipitation on Bermuda. *Tellus, 40B*, 463–479.

Piel, C., Weller, R., Huke, M., & Wagenbach, D. (2006). Atmospheric methane sulfonate and non-sea-salt sulfate records at the European Project for Ice Coring in Antarctica (EPICA) deep-drilling site in Dronning Maud Land, Antarctica. *Journal of Geophysical Research, 111*, D03304. doi:10.1029/2005JD006213.

Qu, W. J., Zhang, X. Y., Arimoto, R., Wang, D., Wang, Y. Q., Yan, L. W., et al. (2008). Chemical composition of the background aerosol at two sites in southwestern and northwestern China: Potential influences of regional transport. *Tellus, 60B*, 657–673.

Qu, W. J., Zhang, X. Y., Arimoto, R., Wang, Y. Q., Wang, D., Sheng, L. F., et al. (2009). Aerosol background at two remote CAWNET sites in western China. *Science of the Total Environment, 407*, 3518–3529.

Salam, A., Bauer, H., Kassin, K., Ullah, S. M., & Puxbaum, H. (2003). Aerosol chemical characteristics of a mega-city in Southeast Asia (Dhaka-Bangladesh). *Atmospheric Environment, 37*, 2517–2528.

Salma, I., Chi, X. G., & Maenhaut, W. (2004). Elemental and organic carbon in urban canyon and background environments in Budapest, Hungary. *Atmospheric Environment, 38*, 27–36.

Seinfeld, J. H., Carmichael, G. R., Arimoto, R., Conant, W. C., Brechtel, F. J., Bates, T. S., et al. (2004). ACE-ASIA: Regional climatic and atmospheric chemical effects of Asian dust and pollution. *Bulletin of the American Meteorological Society, 85*, 367–380.

Smith, D. J., Harrision, R. M., Luhana, L., Pio, C. A., Castro, L. M., Tariq, M. N., et al. (1996). Concentrations of particulate airborne polycyclic aromatic hydrocarbons and metals collected in Lahore, Pakistan. *Atmospheric Environment, 30*, 4031–4040.

Stohl, A. (1998). Computation, accuracy and applications of trajectories—A review and bibliography. *Atmospheric Environment, 32*, 947–966.

Tang, J., Wen, Y. P., Zhou, L. X., Qi, D. L., Zheng, M., Trivett, N., et al. (1999). Observational study of black carbon in clean air area of western China. *Quarterly Journal of Applied Meteorology, 10*(2), 160–170 (in Chinese).

Tanner, R. L., Parkhurst, W. J., Valente, M. L., & Phillips, W. D. (2004). Regional composition of PM2.5 aerosols measured at urban, rural and "background" sites in the Tennessee valley. *Atmospheric Environment, 38*, 3143–3153.

Taylor, S. R., & McLennan, S. M. (1995). The geochemical evolution of the continental crust. *Reviews of Geophysics, 33*, 241–265.

Turpin, B. J., & Huntzicker, J. J. (1991). Secondary formation of organic aerosol in the Los Angeles Basin: A descriptive analysis of organic and elemental carbon concentrations. *Atmospheric Environment, 25A*, 207–215.

Venkataraman, C., Reddy, C. K., Josson, S., & Reddy, M. S. (2002). Aerosol size and chemical characteristics at Mumbai, India, during the INDOEX-IFP (1999). *Atmospheric Environment, 36*, 1979–1991.

Wang, G. C., Wen, Y. P., Kong, Q. X., Ren, L. X., & Wang, M. L. (2002). CO_2 background concentration in the atmosphere over the Chinese mainland. *Chinese Science Bulletin, 47*(14), 1217–1220.

Wang, T., Wong, C. H., Cheung, T. F., Blake, D. R., Arimoto, R., Baumann, K., et al. (2004). Relationships of trace gases and aerosols and the emission characteristics at Lin'an, a rural site in eastern China, during spring 2001. *Journal of Geophysical Research, 109*, D19S05.

Xu, J., Bergin, M. H., Yu, X., Liu, G., Zhao, J., Carrico, C. M., et al. (2002). Measurement of aerosol chemical, physical and radiative properties in the Yangtze delta region of China. *Atmospheric Environment, 36*, 161–173.

Zhang, X. Y., Gong, S. L., Arimoto, R., Shen, Z. X., Mei, F. M., Wang, D., et al. (2003). Characterization and temporal variation of Asian dust aerosol from a site in the northern Chinese deserts. *Journal of Atmospheric Chemistry, 44*, 241–257.

Zhang, X. Y., Zhuang, G. S., & Yuan, H. (2004). The dried salt-lakes saline soils sources of the dust storm in Beijing: The individual particles analysis and XPS surface structure analysis. *China Environmental Science, 24*(5), 533–537 (in Chinese).

Zhou, L. X., Worthy, D. E. J., Lang, P. M., Ernst, M. K., Zhang, X. C., Wen, Y. P., et al. (2004). Ten years of atmospheric methane observations at a high elevation site in western China. *Atmospheric Environment, 38*, 7041–7054.